SPE 71695

Geomechanical Analysis and Decision Analysis for Mitigating Compaction Related Casing Damage

Michael S. Bruno, SPE, Terralog Technologies USA, Inc.

Abstract

Reservoir compaction and associated bedding plane slip and overburden shear has induced damage to hundreds of wells in oil and gas fields throughout the world. Critical casing damage mechanisms observed in a variety of structural settings include: 1) overburden shear damage on localized horizontal planes; 2) shearing at the top of production and injection intervals; and 3) compression and buckling damage within the production interval primarily around perforations.

Analytical solutions are readily available to estimate compaction, subsidence, and casing damage risks. These should be applied as initial screening tools at an early stage in reservoir development planning. They can also be applied to estimate relative risks for various well locations and trajectories.

Geomechanical models of increasing complexity, including two-dimensional and three dimensional finite element type techniques have been used with good success to assess formation deformation and casing damage risks in several reservoirs, and are described herein. Three dimensional geomechanical models at the wellbore scale are required to evaluate shearing deformation on specific well designs, and are used to assess damage mitigation effectiveness for varying completion strategies.

An economic decision tree model is applied to compare the costs and benefits of alternative well designs, while taking into account inherent uncertainties in model input data, well damage location, and the effectiveness of various mitigation strategies. In some instances the appropriate action is not to change completion design and simply accept damage risk.

Introduction

Significant subsidence and casing damage have occurred at several fields throughout the world, including the North Sea, in the Gulf of Mexico, in California, Canada, South America, and Southeast Asia[1-10]. Problems can be particularly acute in deep offshore operations, where individual well costs often exceed 10million dollars and specific wells often target individual sand formations or fault blocks. Hence the loss of even one or two wells may significantly impact recoverable reserves for the field.

Compaction related casing damage can include compression and buckling, localized shearing deformation, tension damage, and even distortion damage to internal completion assemblies such as pre-packed screens. The appropriate mitigation strategy will depend on the most likely location of casing damage, the expected type of damage, and the damage magnitude. This requires combining geomechanical analysis of deformations in the reservoir, overburden, and the casing-cement-formation assembly with quantitative decision analysis that compare the costs of various mitigation strategies to the economic benefit of reducing damage risk, given the inherent uncertainty and variability in reservoir deformation, damage type and location, and mitigation effectiveness.

This paper describes casing damage observations worldwide and geomechanical analysis techniques applied to evaluate casing damage mitigation strategies. We further describe a quantitative decision analysis process to estimate the economic value of various completion designs to mitigate casing damage.

Compaction and Subsidence Overview

The weight of sediments above an oil and gas bearing geologic formation is supported partially by the rock matrix and partially by the pressurized fluid or gas within the rock pore space. When fluid pressure is reduced, more of the load is transferred to the rock matrix and the pressure-depleted formation compacts slightly. Subsurface compaction, if it is significant or if the formation is relatively shallow, can produce measurable surface subsidence. Formation compaction can induce compression and buckling damage within the producing interval. More importantly, significant formation compaction also induces small-scale slip on bedding

planes and faults within the reservoir and overburden material, causing severe shear damage to wells.

Formation Compaction. The effective stress on a porous material is equal to external stress applied to the material minus the internal pore pressure. For geologic formations, the vertical external stress is the weight of overburden material while the lateral stress will depend on the tectonic setting. External stresses generally remain constant while the internal pore pressure declines during fluid withdrawal or increases with fluid injection. A change in effective stress leads to volume compression, which is equal to the change in pore pressure times the compressibility property for the material. A reservoir formation subject to pore pressure change will compress uniformly or uniaxially depending on loading pattern and geometry. A general change in bulk volume, V, is related to the bulk compressibility, Cb, and pore pressure change, ΔP, through the expression:

$$\Delta V / V = Cb\Delta P \qquad (1).$$

For most oil and gas formations, however, the lateral dimensions of the formation are large relative to the formation thickness. Furthermore, while the surface above the formation is completely free to displace downwards, lateral deformation is constrained by adjacent material. Therefore, most of the compression associated with pressure decline in relatively thin, flat lying, geologic formations occurs in the vertical direction. The magnitude of this vertical compaction or pressure-induced change in formation thickness, ΔH, can be estimated by the following equation:

$$\Delta H / H = Cm \, \Delta P \qquad (2),$$

where H is the original formation thickness, Cm is the uniaxial compaction coefficient for the material, and ΔP is the change in pore pressure. For elastic and isotropic materials, and assuming grain compressibility is small relative to bulk compressibility, the uniaxial compaction coefficient is related to the bulk compressibility through the expression:

$$Cm = (1+\nu)Cb/3(1-\nu) = 1/\rho V_c^2 \qquad (3),$$

where ν is the Poisson's Ratio for the material, ρ is the bulk density, and V_c is the compressional wave velocity for the formation material.

Equations (1) through (3) may be used to approximate formation compaction for a given pressure decline and compressibility. These equations assume uniform formation thickness, uniform pressure decline, and elastic isotropic material behavior. In most geologic settings formation thickness varies and material behavior is pressure dependent and non-isotropic, so that more sophisticated geomechanical models are required for accurate analysis. However, these equations do provide useful order of magnitude estimates for reservoir compaction.

Surface Subsidence. If subsurface formation compaction is significant it will induce both vertical surface displacements (subsidence) and horizontal surface displacements. The amount of surface subsidence is primarily related to the magnitude of the formation compaction, its lateral extent, and the formation depth. Deeply buried formation compaction of limited areal extent will induce almost no surface subsidence, while laterally extensive or relatively shallow formations can induce surface subsidence nearly equal to the subsurface compaction. The lateral extent of surface subsidence is also related to the depth of the subsurface compaction zone.

Analytical equations are available to estimate surface subsidence when the subsurface compaction zone is of uniform shape. Generally, these are based on nucleus-of-strain equations from continuum mechanics described by Sen and Geertsma[9,14] For example, given a roughly disk shaped oil and gas bearing formation with compaction coefficient Cm and Poison's Ratio, ν, average radius, R, average thickness, H, and depth of burial, D, the maximum vertical subsidence, S, can be estimated with the following equation[1]:

$$S = 2Cm(1-\nu)[H - (R^2+(D+H)^2)^{0.5} + (R^2+D^2)^{0.5}]\Delta P \qquad (4).$$

Equation (4) above is valid when the subsurface compaction zone is uniform and when the overburden material deforms elastically and homogeneously. The elastic overburden deformation assumption is usually valid. For example, consider a formation compacting a total of 10m even at a relatively shallow depth of 1000m. The overburden material will deform a maximum of 10m in the vertical direction over its 1000m thickness, and generally much less, so that strains will be less than 1% and elastic material behavior assumptions are reasonably accurate. Furthermore, for a given amount of subsurface compaction, resulting surface subsidence is relatively insensitive to overburden material properties, so that analytical nucleus of strain equations actually provide very good subsidence approximations to even the most sophisticated geomechanical models which account for inelastic and heterogeneous overburden behavior (within about 20%). More sophisticated models are usually only required to account for the formation compaction itself, or to accurately evaluate deformations and stresses within the overburden (to assess casing damage risk, for example).

Next we consider the pattern of deformation within and above compacting formations and the resulting implications for casing damage. Figure 1 presents a geomechanical simulation for a flat lying geologic formation, with lateral extent approximately equal to burial depth, subject to uniform pressure decline, and with overlying bedding planes susceptible to slip due to varying material properties. The formation itself compacts nearly uniformly, leading to risks for compression and buckling damage. Overburden layers exhibit shear slip, leading to risks for localized shear damage to wells, and the surface above the formation subsides over a lateral extent beyond the edge of the subsurface compacting formation. In the following sections we discuss the resulting well casing damage mechanisms.
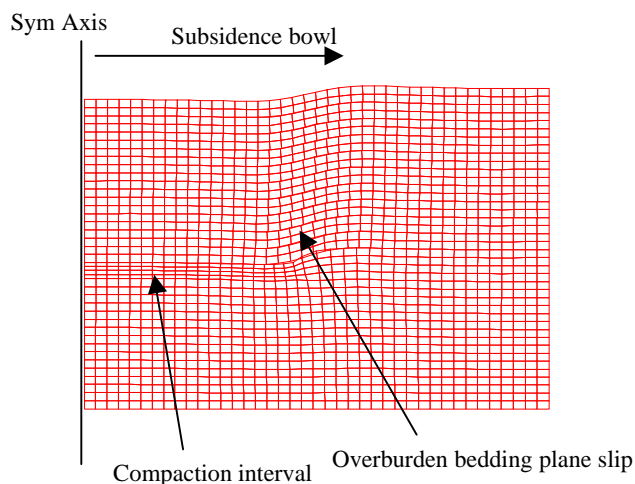
Figure 1.   Sample formation compaction, overburden shear, and surface subsidence patterns induced by pressure depletion.

Casing Damage Mechanics

Terralog Technologies has analyzed compaction and casing damage observations worldwide as the principal investigator for a 3-yr Joint Industry Project focussed on compaction induced casing damage (Drilling Engineering Association Project DEA99), as a contractor on several Department of Energy sponsored research projects, and through more than a dozen private company sponsored projects.   These investigations have provided important insights on basic well casing damage mechanisms. There are three critical forms of well damage that have been observed in almost all settings. These are:

1. Localized horizontal shear at weak lithology interfaces within the overburden;

2. Localized horizontal shear at the top of production and injection intervals; and,

3. Casing compression and buckling damage within the producing interval, primarily located near perforations.

Overburden Shear Damage. Localized shear deformation at weak layers within the overburden appears to have occurred in almost every field investigated. Specific examples of this type of damage have been noted by Poland and Davis[12] at the Wilmington Field in California, by Bruno[2] and by Fredrich et al[7,8] at the Belridge and Lost Hills Fields in California, and by Yudovich, Schwall, and others[13,15] at the Ekofisk field in the North Sea.

One key feature of this type of damage is that shearing deformations tend to be localized over a relatively short length of casing, on the order of only several feet. This is clearly demonstrated in various caliper images, such as the example presented in Figures 2 from a field in Southeast Asia. Although there is often uncertainty on the quantitative nature of caliper measurements, the basic observations are accurate and have been confirmed in recovered casing sections. To

illustrate the localized nature of these overburden deformations, we can refer to a photo of an actual section of recovered casing damaged at the Wilmington field shown in Figure 3 (from Frame, 1952)[6]. The photo demonstrates that about 10 inches of shear displacement occurred over a length of less than 5 feet, a pattern consistent with caliper measurements at the Ekofisk and Valhall fields in the North Sea, and with gyro and inclinometer surveys at the Belridge field in California and the Cold Lake field in Alberta.
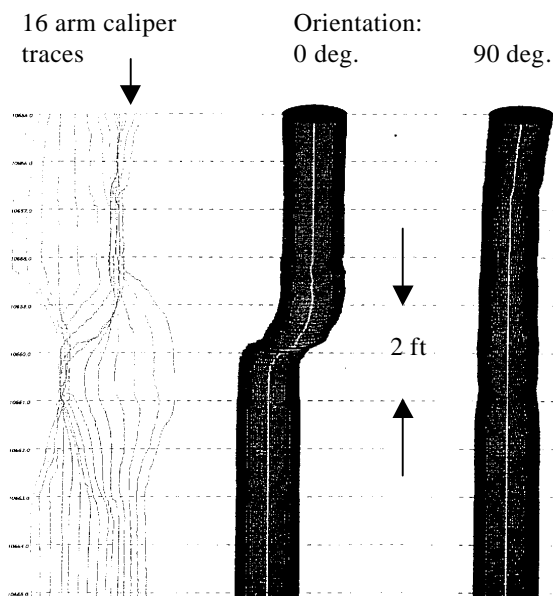

Figure 2.   Sample casing deformation pattern noted in caliper logs for damaged gas well (9.62" casing) in Southeast Asia.
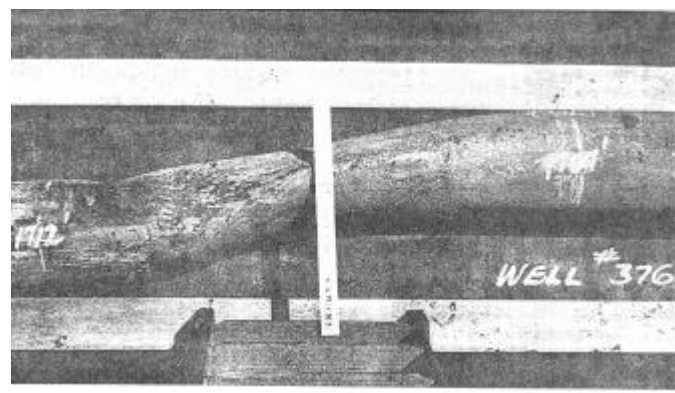

Figure 3. Localized deformation in well damaged within overburden at Wilmington Field.   About 10" lateral offset on 10¾" casing from 1707ft to 1712ft depth. (From Frame, 1952).

The location of overburden damage is often related to weak layers, rather than to areas of high induced shear stress. This is perhaps a subtle point. Certainly the compaction-induced shear stresses are the driving force for damage, but the location of failure is dictated more strongly by the location of weak interfaces rather than by the location of high shear stress. This conclusion is supported by several observations. First, induced shear stresses in the overburden tend to be distributed over relatively large depth intervals (see for example, Bruno, 1990)[1]. By contrast, the observed overburden damage is sometimes (although not always) very localized with depth. Second, overburden damage does not occur exclusively towards the flanks of the developing subsidence bowl where compaction induced shear stresses are highest. Although well damaged in the overburden did concentrate around the reservoir flanks at Ekofisk (see Figure 4), and to some extent at Wilmington, experiences at Valhall, Arun, Belridge, Lost Hills, and Cold Lake suggest that overburden shearing damage is often more widely distributed.
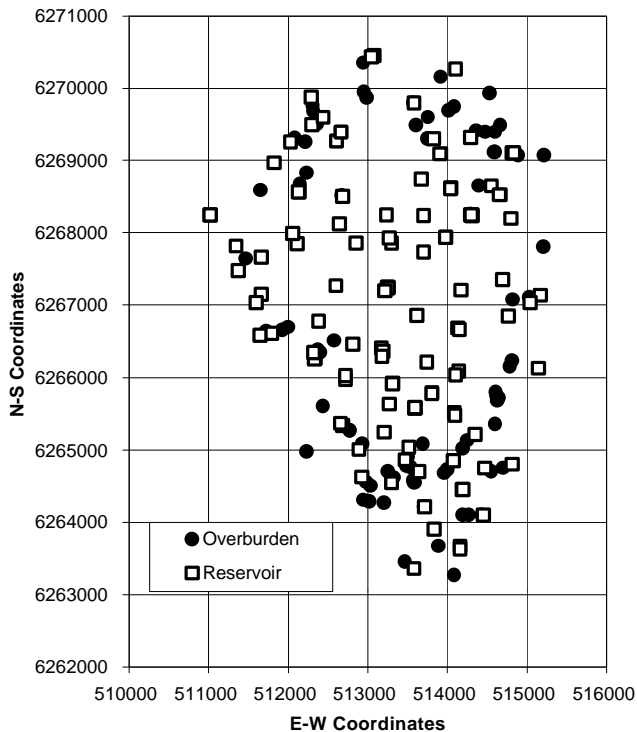

Figure 4. Distribution of wells damaged in overburden and within the reservoir at Ekofisk. Overburden damage was initially concentrated along flanks of the field where shear stresses are highest.

Observations of well damage at Belridge in particular demonstrate that with extensive development and compaction, localized shear damage at weak overburden layers can be very widely distributed over all portions of the field[4,7,11].

Such observations raise important implications for mitigation strategies. Potential weak interfaces should be identified for new developments with high compaction risk through detailed formation evaluation techniques. Although shear damage mitigation strategies such as under-reaming should be concentrated in flank areas, with continued development it is not always safe to assume that this will be sufficient for continuing development strategies. Finally, as has been noted at Belridge and Cold Lake, once slip has occurred on weak overburden layers, then additional slip can be induced by either production or injection operations (reverse slip).

Shearing at Top of Producing Interval. A second common and critical damage mechanism noted at many fields involves localized shear damage near the top of the producing interval. This was noted in particular at the Belridge and Cold Lake fields, and perhaps to a lesser extent at Ekofisk, Valhall, and the Arun field in Indonesia. The driving mechanism appears to be a combination of vertical movement of the underlying formation and differential lateral contraction (or expansion during injection) of the producing formation relative to the capping shale. That is, the producing formations are typically more permeable and soft (due to higher porosity) than the capping shale. The contrast in pressure change and stiffness leads to differential lateral expansion and interface slip.

This shear deformation induced by contrasts in lateral displacement is a fundamentally different shear mechanism than slip induced by distributed overburden shear stresses related to reservoir compaction. It is also often associated with injection operations. The impact on well casings, however, is quite similar to shear higher within the overburden. Nearly horizontal shearing is developed over a very localized zone. The magnitude of shear (several inches) and localization are clearly documented in caliper and inclinometer surveys conducted at Cold Lake (see for example Gronseth, 1990)[10].

An increased concentration of well damage at the top of the producing and injection interval is also clearly seen at the Belridge field after the initiation of extensive waterflooding (shown in Figures 5 and 6). Water injection did help to reduce compaction, surface subsidence, and the total number of well failures. But it also led to an increased percentage of damage at the top of the production and injection formation in comparison to damage higher within the overburden.
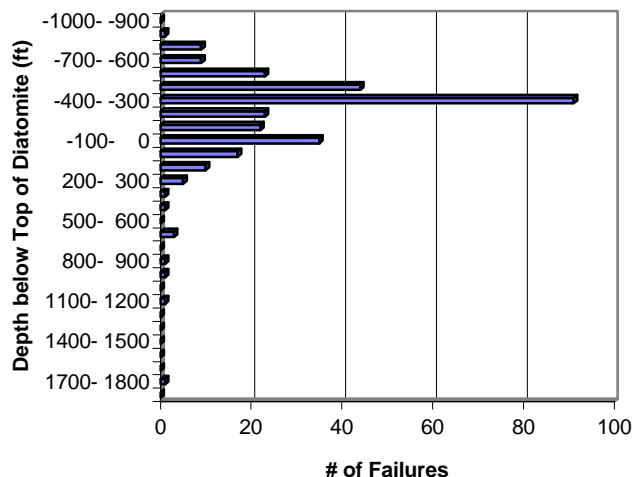
Figure 5. Vertical distribution of well damage at Belridge field before 1990.
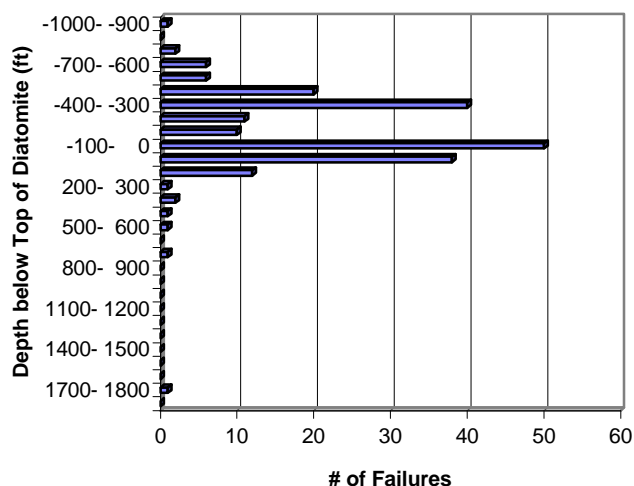

Figure 6. Vertical distribution of well damage at Belridge field after extensive waterflooding beginning around 1990

Such formation shear mechanisms are most dominant for relatively shallower reservoirs. In these situations the overburden load at the top of the producing interval, which provides the normal force resisting shear deformation, is of lower magnitude than for very deep reservoirs.

For deviated wells, damage caused by this lateral shear at the top of the producing interval can be exacerbated by vertical compaction of the producing formation, which can add additional local casing compression or bending. This has been noted at the Cold Lake field, in which wells deviated at an angle of 30 degrees or more from vertical experienced

nearly twice the rate of failure at the top of the production/injection zone than vertical wells.

Compression and Buckling Damage. The third critical casing damage mechanism noted in almost all the fields examined is axial compression and buckling within the producing interval. This has been observed to occur most frequently near perforated intervals, and is related to formation compaction induced by pressure decline. Axial buckling is most severe in vertical wells. Observations of this type have been noted most clearly at Ekofisk, Belrdige, Lost Hills, and Valhall, and in several Gulf of Mexico formations.

The reason axial buckling is observed most often near perforated intervals is twofold: first, these are the zones experiencing the most severe pressure drawdown and compaction; and second, these are the areas in which solids production can lead to loss of lateral support. In fact, it is nearly impossible to induce axial buckling on a casing string whenever there is good cement coverage and formation support (see analysis in Bruno, 1992)[1].

Mitigation Strategies. The appropriate mitigation strategy for a given well trajectory will depend on the most likely location of casing damage, the expected type of damage, and the damage magnitude. Buckling damage is most effectively mitigated by ensuring a good cement bond around the casing and by reducing solids production. Compression damage can be mitigated by increasing the thickness to diameter ratio of selected casing. The most effective mitigation strategy to reduce localized shear damage, however, is to accommodate lateral deformation through hole size, casing diameter, and cementing practices; strengthening the casing is almost useless.

Another technique to mitigate casing damage is to avoid high shear stress areas near the top of the producing formation and within the overburden, and to adjust the deviation angles of wells to minimize axial compression or transverse shear. This generally requires geomechanical modeling of the reservoir and overburden to identify stress magnitudes and patterns induced by pressure depletion.

Many (although not all) mitigation strategies required to avoid or reduce well damage increase well drilling and completion costs. The question then becomes: is the additional cost for such changes justified by the benefits of damage mitigation, given the inevitable uncertainties? Drilling costs are often controlled and borne by drilling departments and engineers, while subsequent well damage and lost production costs are sometimes only recognized and borne by production departments and engineers several years later. Hence a strong argument, supported by quantitative analysis, is generally required to justify expending additional upfront drilling funds to avoid future production losses or redrill costs.

Answering this question often requires combining geomechanical analysis of the formation and casing assembly with quantitative decision analysis. One can then compare the costs of various mitigation strategies to the economic benefit of reducing damage risk, given the inherent uncertainty and

variability in reservoir deformation, damage type and location, and mitigation effectiveness.

Geomechanical Analysis Techniques

Several geomechanical analysis techniques of varying complexity are available to analyze reservoir deformations and associated casing damage risks.   These include elastic analytical equations with simple geometric approximations, more detailed elastic solutions allowing discretization of the reservoir in three dimensions and deformation analysis on arbitrarily oriented well trajectories, and two dimensional or three dimensional finite element type models incorporating complex constitutive behavior for formation materials, casing configurations and cementing strategies.   The appropriate approach will depend on the analysis goals (for example an estimate of subsidence or an estimate of casing damage), the mitigation options to be considered (for example changing completion design, well trajectory, or reservoir development strategy) and the availability of data. We will discuss in turn several techniques requiring increasing effort and input data.

Simple Analytical Solutions.   Simple analytical solutions should always be applied during the initial screening phase to assess the relative significance of subsidence or casing damage risks for a given field. For example, equations (1) through (3) provide a quick order of magnitude assessment of compaction and subsidence magnitude and require only approximate estimates of reservoir geometry and formation properties.

Casing compression and buckling damage risks can then be estimated by considering compressive strains induced on wells penetrating the compacting formation at various deviation angles.   The worse case scenario assumes that all of the formation compaction is transferred to the well casing; that is, that there is no slip or shearing occurring at the casing-cement or cement-formation interfaces.   Then the axial strain on the casing will be equal to the effective vertical formation compaction (taking into account net sand and shale volumes) transformed into the well deviation direction. For example, if a well is deviated at an angle, θ, from vertical through a formation which is compacting in a vertical direction by an amount equal to the uniaxial compaction coefficient Cm times a pressure drawdown, ΔP, the resulting axial compressive strain, ε_c, can be approximated by:

$$\varepsilon_c = 0.5(1+\cos2\theta)Cm\Delta P \qquad (5).$$

Yielding strains for casing steel range from about 0.3% to 0.7%, depending on grade. Compressive deformation on the order of 1% or less, however, is relatively mild and will not impair the casing integrity or functionality.

The critical buckling strain (defined as the onset of instability) for a casing string with fixed ends and unsupported over a length, L, may be expressed as:

$$\varepsilon_{\text{critical-unsupported}} = 4\pi^2 I/(AcL^2) \qquad (6),$$

where I is the moment of inertia for the casing cross section (= $R^3 t$) and Ac is the cross section area (=$2\pi Rt$).   If the section of casing is supported, then the critical buckling strain will depend on the relative ratio of the formation stiffness modulus and the casing Young's modulus.   A conservative approximation to the critical buckling strain can be expressed as (Bruno, 1990):

$$\varepsilon_{\text{critical-supported}} > (2/Ac)(2E_f I/E_c)^{0.5} \qquad (7),$$

where E_f is the formation material Young's Modulus. For example, the critical buckling strain for 9 5/8 inch, 53 lb/ft, casing unsupported over a 10ft length would be on the order of 0.9% while the critical buckling strain for the same casing supported by formation material with Young's Modulus on the order of 1.0E5 psi would be about 7.5% (i.e. well above the level for localized compression damage).

Vertical formation compaction acting on a deviated wellbore will also induce shearing deformations and kinking of the casing string where it enters and exits the formation sand. The shear strain on the casing, γ_c, can be approximated by:

$$\gamma_c = 0.5(\sin2\theta)Cm\Delta P \qquad (8).$$

If a producing sand compacts while the overlying and underlying formations do not, then the formation compaction will produce kinking of the casing at the formation entry and exit points.   The kink angle is related to the change in formation thickness ΔT, the original thickness, T, and the deviation angle, θ, according to the following approximation:

$$\text{Kink Angle} = \tan^{-1}\{T\tan\theta/(T-\Delta t)\} - \theta \qquad (9).$$

In a similar manner we can estimate potential risks for bedding plane slip at the top of the production interval and within the overburden material. For a first approximation we consider analytical solutions for stresses induced in an elastic half-space due to nuclei of compression distributed over the formation volume[9,15].   The assumptions are that the overburden material behaves in a linear elastic, isotropic, and homogeneous manner. For example, the total induced shear stresses caused by a varying pressure within an arbitrarily shaped reservoir can be obtained by integrating the contribution of all the compaction points over the reservoir volume, V, as follows:

$$t_{yz}(x_0,y_0,z_0) = \frac{C_b E_0}{12\pi(1-n)}\int_V \Delta P(x,y,z)\left[\frac{\partial^2 V_1}{\partial y \partial z} + 2z\frac{\partial^3 V_2}{\partial y \partial z^2} + \frac{\partial^2 V_2}{\partial y \partial z}\right]dV$$

$$t_{xz}(x_0,y_0,z_0) = \frac{C_b E_0}{12\pi(1-n)}\int_V \Delta P(x,y,z)\left[\frac{\partial^2 V_1}{\partial x \partial z} + 2z\frac{\partial^3 V_2}{\partial x \partial z^2} + \frac{\partial^2 V_2}{\partial x \partial z}\right]dV$$

$$(10).$$

In the expression above τ_{xz} and τ_{yz} are the horizontal shear stresses at position (x_0, y_0, z_0). E_o is the Young's Modulus for the overburden material and ν is the Poisson's ratio for the reservoir and overburden. V_1 and V_2 are distance functions given by:

$$V_1 = \frac{1}{\sqrt{(x - x_0)^2 + (y - y_0)^2 + (z - z_0)^2}} \quad (11),$$

$$V_2 = \frac{1}{\sqrt{(x - x_0)^2 + (y - y_0)^2 + (z + z_0)^2}} \quad (12).$$

The change in pressure, $\Delta P(x,y,z)$, is measured from some reference state (usually the normal reservoir pressure) from which induced stresses are to be determined. Equations (11) and (12) above may be integrated analytically if the pressure distribution is a simple function, or numerically if pressures are obtained from a simulation model. Induced shear stresses are most severe when the pressure decline is uniform and ends abruptly at the reservoir boundary, such as with fault bounded reservoirs. Shear stress magnitudes increase with larger radius to depth ratio. However, once a reservoir is deeper than about the distance of its radius, shear stress magnitude are relatively unaffected by depth, and are controlled primarily by the ratio of reservoir thickness to reservoir radius.

To estimate maximum formation shear stress we might assume that pressure decline is constant throughout the volume of the reservoir, and evaluate stresses where they are largest: at the top and flank edge of the producing formation. These estimates for maximum horizontal shear stress at the top of the producing formation may be compared to the normal effective stress and friction coefficient for the material to investigate bedding plane slip risks. For example, we can assume that slip may occur according to a Coulomb type friction criterion of the form:

$$\tau > So + \mu\sigma_v \quad (13),$$

where τ is the horizontal shear stress, So is the material cohesion, μ is the friction coefficient, and σv is the effective vertical stress on the horizontal plane.

Equations (4) through (13), or similar approximations, may be applied with worst-case assumptions regarding reservoir geometry, pressure depletion, and material properties to determine if compaction and casing damage risk are potential problems. The next step in the process would be to determine where damage risk is most likely to occur. This can be done by extending the analytical solutions to more complex reservoir geometries and well trajectories.

Three-dimensional elastic models. The analytical equations discussed above provide order of magnitude estimates for compaction, subsidence, and shear stresses at single points above simply shaped reservoirs. More detailed solutions are required to account for actual reservoir geometry and to provide information regarding distributed stresses or displacements in the subsurface.

We can develop a relatively simple three dimensional model by discretizing a producing horizon into grid elements and treating each cell as either a nucleus of strain or a displacement discontinuity in an elastic half-space. Reservoir element deformations are assumed to be related to the change in fluid pressure times the average element thickness times the compaction coefficient. Analytical functions, of the type given in equation (9) are then used to determine displacements, strains, or stresses at any point in the half space by superimposing the influences from all reservoir elements. If necessary, a step-wise linearization procedure can be applied to evaluate non-linear and time dependent overburden property behavior.

The method can then be applied to estimate, for example, induced displacements along proposed well trajectories, induced stresses on known fault planes, or induced shear strains on a given horizon. It is particularly useful to use the same grid assembly for geomechanical analysis as used in reservoir simulation, so that flow simulation pressure results can be applied directly to drive the geomechanical model (one-way flow-geomechanical coupling).

This approach is illustrated in a sample geomechanical analysis to evaluate subsidence and shear damage risks for an offshore gas reservoir. Figure 7 presents the gas formation isopach used to discretize the reservoir into an assembly of grid blocks. Vertical displacements at the seafloor, shown in Figure 8, and horizontal shear strains at a depth of about 1650m below the mudline, shown in Figure 9, are both estimated using influence functions for dipping tensile displacement discontinuities in an elastic half-space. The resulting surface subsidence contours were used to help assess platform placement and design criteria, while the subsurface shear deformation patterns were used to select low-risk well trajectories.
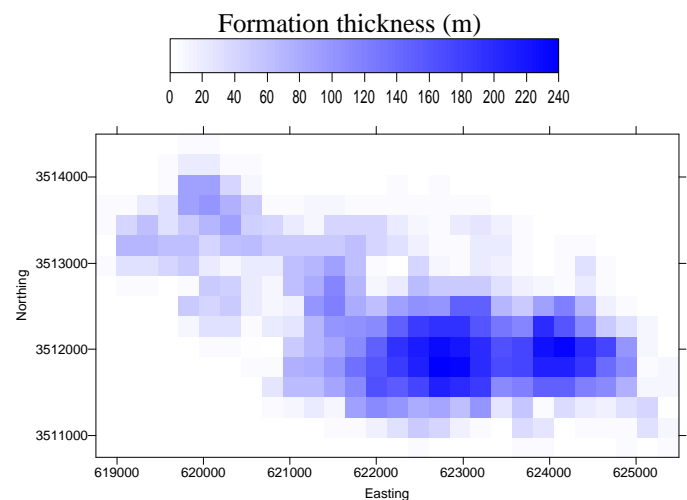

Figure 7.   Discretization of an offshore gas field for 3D displacement discontinuity modeling.
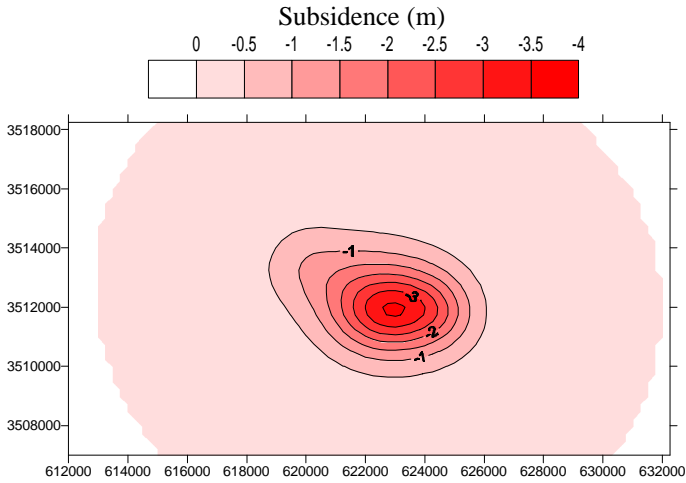
Subsidence (m)

Figure 8.   Resulting surface subsidence pattern for uniform depletion seenario.
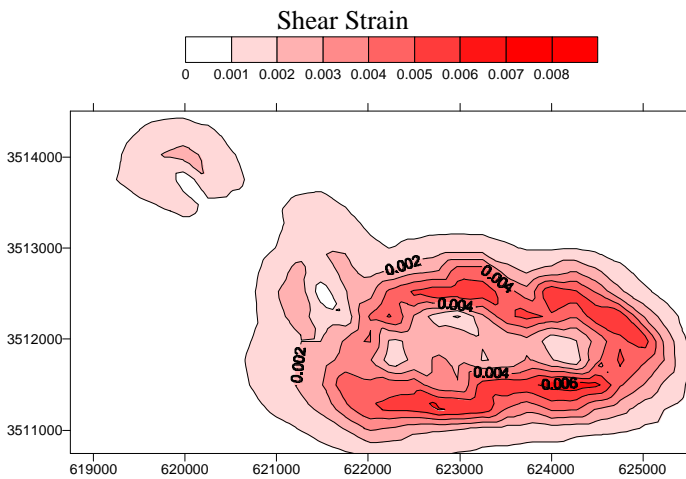
Shear Strain

Figure 9.   Resulting shear strain pattern at 1650m depth for uniform depletion scenario.

Such solutions are quantitative in nature. They can account for inelastic formation compaction through appropriate compressibility vs. pressure relations, but they require that overburden deformations remain elastic and homogeneous. Hence they can simulate overburden deformations up to the point of failure (such as to incipient faulting or bedding plane slip, but not beyond that point. They are sufficiently accurate to identify areas of relative high risk vs. low risk, for example to help select well trajectories, but they are not accurate enough (especially in the producing

horizon) to provide quantitative displacement and stress magnitudes for analyzing appropriate casing design and completion designs for a specific well location. That level of accuracy requires finite element type techniques to account for heterogeneous material layers with inelastic constitutive behavior, as summarized in the following sections. It also requires material property data, typically from core analysis, for input data.

Two-dimensional numerical modeling. The analytical influence function techniques discussed above are simple to apply and very computationally efficient because they only require discretization of the reservoir. For greater accuracy, however, both the reservoir and the overburden material must be discretized and modeled in either two dimensions or three dimensions.

The next incremental level of modeling complexity is to assume the reservoir response is sufficiently symmetric and uniform about one axis so that a reasonable approximation can be achieved with a single slice through through the field. This might be the case, for example, if one structural axis is elongated and well development is extensive throughout the field. Alternatively, one might evaluate multiple slices at various locations or even at orthogonal directions across a structure and evaluate a range of responses to bracket the solution.

A two-dimensional geomechanical model, therefore, can be used to accurately account for structural effects in one direction, to account for vertical layering and heterogeneity, and to account for inelastic material behavior. The appropriate orientation for the 2D model is often guided by insights gained from a 3D analytic solution (such as that shown in Figures 7, 8, and 9). Two dimensional models of this type have been used with good success to accurately match field observations for surface subsidence and to qualitatively investigate casing damage risks for varying injection and production strategies (see for example Bruno and Bovberg, 1992; Hansen et al, 1995; Hilbert et al, 1996)[1,2,3].

We illustrate this process with a field example from California. Figure 10 presents a two-dimensional cross section mesh across an oilfield in California, using the FLAC2D geomechanical model. The model extends 6000 feet in the horizontal direction and 5000 feet in the vertical direction, and comprises 4235 elements. The structural geology is accurately captured by incorporating geologic marker data from several wells across the section. The overburden is represented by 30 layers with 5 different material properties, the reservoir formation is represented by 10 layers with 3 different material properties, and the underburden is represented by 10 layers with a single material property. The overburden and reservoir response are simulated with inelastic, strain-softening, material models matched to measured triaxial test data on cores. Potential bedding plane slip surfaces were placed at the top of the producing horizon and at shallower depth within the overburden, consistent with observed casing damage in other parts of the field.
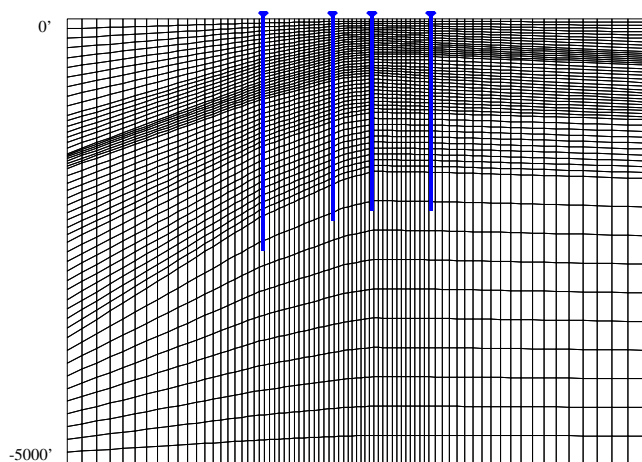
Figure 10.   Two-dimensional cross section model to investigate compaction and well damage in a California oilfield.
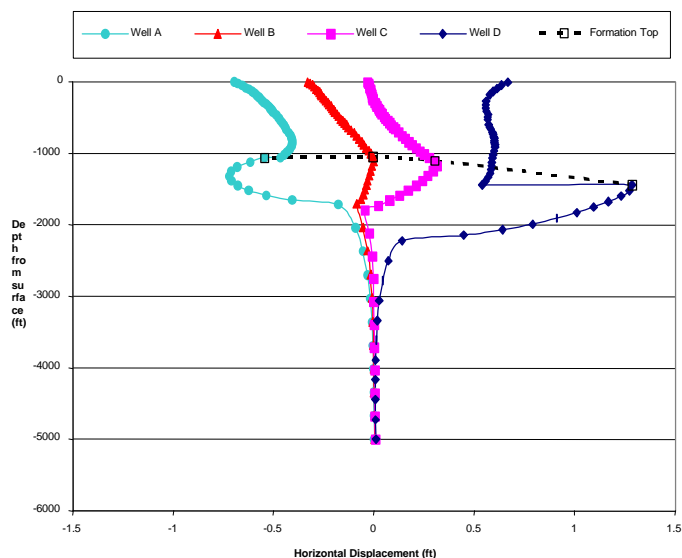

Figure 11.   Horizontal displacements vs. depth induced on several well trajectories by reservoir compaction.

Figure 11 presents the horizontal displacements along several well trajectories induced by uniform depletion of the producing horizon. The simulation indicates relatively minor deformation and kinking of well casings on one edge and within the center of the field, but more severe shear damage risk on towards the other edge of the field. Additional simulations were performed under varying depletion scenarios and for a range of material properties to assess subsidence and casing damage risks.

Three-dimensional reservoir modeling

The final level of complexity is to fully discretize the reservoir and overburden in three dimensions.   Such a model can then account for 3D structural effects and for production and injection patterns that vary across a field, thereby introducing non-uniform and non-symmetric displacement patterns.   Very large scale three-dimensional models (on the order of several hundred thousand grid blocks) have been developed to analyze subsidence and casing damage risks for varying production scenarios at several fields in the US (see Fredrich et al, 1996; 2001)[7,8].   For example, Figure 12 presents the mesh of approximately 260,000 elements generated by Terralog from geologic marker data and applied by Sandia National Laboratories to analyze subsidence and casing damage at the Lost Hills Field [8].
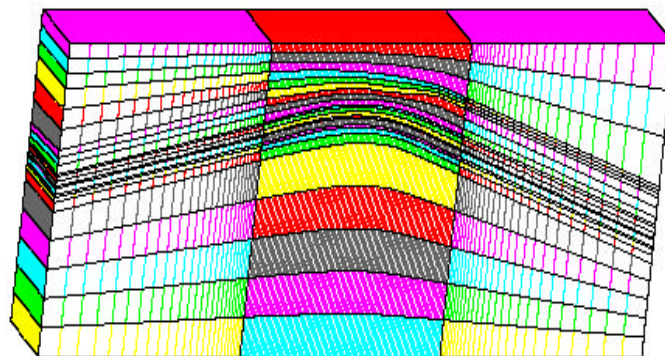

Figure 12.   Large-scale three-dimensional finite element model to investigate compaction and casing damage at the Lost Hills field[8]

In the model shown above, one-way fluid-flow and geomechancial coupling was achieved by matching the grid in the reservoir formation to a 3-D fluid flow simulation grid. While it is possible to combine fluid-flow equations and geomechanical equations into a single simulator, the combination often compromises accuracy in one area or another. This is a severe drawback to almost all fully coupled geomechanics-fluid flow simulators. The advantages gained by achieving true geomechanical coupling (which has a second order affect on flow) are usually outweighed by the disadvantages of not having an accurate reservoir simulation incorporating first-order effects on flow such as relative permeability, temperature and pressure related phase transitions, and appropriate near wellbore models for skin and productivity.

Three-dimensional wellbore modeling. So far we have restricted our discussion to reservoir-scale models. These are necessary to evaluate the displacements (including compaction and shear deformations) at various locations within and above a producing formation induced by varying production and injection scenarios. One additional key goal, however, is to also assess the effectiveness of different completion designs to avoid or mitigate casing damage at a given location. This requires detailed modeling at the near-wellbore scale.

It is numerically impractical to combine very large-scale reservoir model elements (on the order of 10s of feet) with very-small scale casing elements (on the order of 10ths of inches) within a single model. Furthermore, it is unnecessary, as the existence of a relatively small diameter casing string through a geologic formation of large lateral extent does not influence the reservoir deformations. Therefore, it is best to discretize the near wellbore region separately to very fine scale, and simply impose the deformation patterns determined from the large-scale model onto this assembly to evaluate near-wellbore casing-cement-formation interaction.

This cannot be simply done in two-dimensions (for example in an axisymmetric simulation), unless vertical compression damage to a vertical well is the only consideration. Three-dimensional models are required to simulate vertical compression on deviated wells and lateral shear displacements transverse to a circular well section. Furthermore, when finite compression and shear deformations are imposed on a casing assembly, the resulting strains are very large and the material behavior is significantly inelastic, so that sophisticated material models are necessary to simulate large displacements and failure of inner completions (if there is one), the casing, the cement, and nearby formation material.

Terralog has analyzed several completion designs to mitigate compression and shear damage for several clients in the US and Europe. For example, Figure 13 presents a deformed model mesh for a deviated well, subject to combined compression and shear. As illustrated in the detail view of Figure 14, the wellbore assembly comprises a centralized inner completion (wire wrapped screen), gravel pack, production casing, surrounding cement, and about 12 feet of surrounding formation material. Inelastic material properties for the formation, cement, and gravel pack are determined from laboratory test data.

The commercial software FLAC3D (Itasca Consulting Group) was used for this geomechanical model because it has a wide range of geologic material models that can be easily modified to incorporate observed inelastic behavior, such as shear failure, compaction failure, and strain softening. The model mesh shown comprises about 80,000 elements, and the motivation is to assess damage risk to the inner completion caused by compression and shear deformations, for varying centralizer and gravel pack screen assemblies.
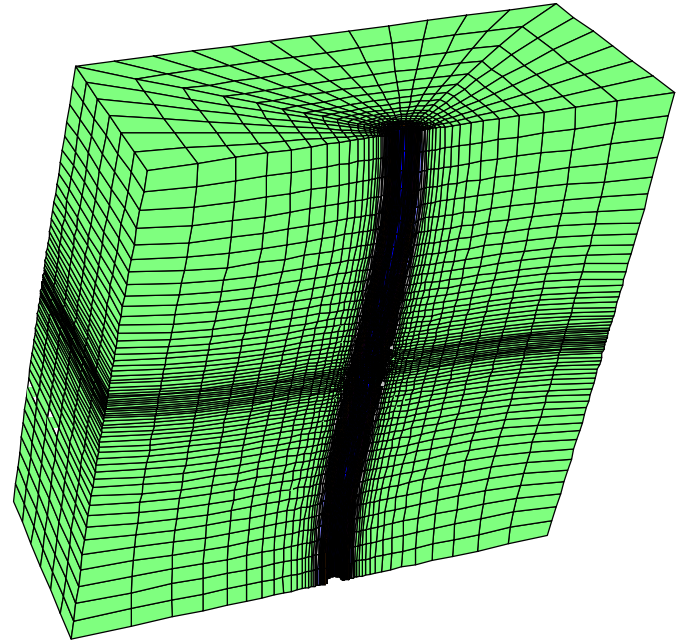

Figure 13. Deformed mesh on three-dimensional near wellbore model to investigate combined compression and shear damage to casings and inner completions.
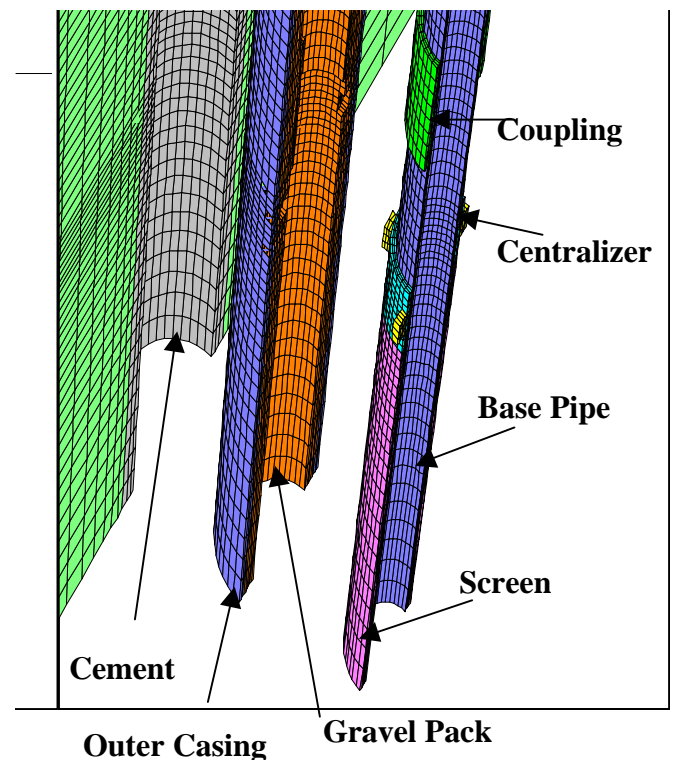

Figure 14. Exploded view of embedded completion assembly

As illustrated dramatically in Figure 3, production casings can often experience significant localized shear deformation without breaching. If this same displacement magnitude is transferred directly to a relatively small diameter and relatively stiff inner completion, however, significant screen damage and coupling breach may occur. Direct load transfer can sometimes be mitigated by adjusting the spacing and design of centralizers and by adjusting the density of fracpack sand in certain areas.   Several other mitigation strategies (such as adjusting well trajectory, modifying cement thickness and ductility, or spacing screen connections) can be evaluated with detailed three-dimensional well models of this type.

Decision Analysis Techniques

After geomechanical analytical techniques or numerical models have been applied to assess compaction and shear deformation risks, and to assess the potential benefits of varying well designs and completion strategies, the final step is to determine if the added benefits outweigh any additional cost.   This cost-benefit analysis must take into account various types of uncertainty, such as uncertainty in material behavior throughout the field, uncertainty in pressure response throughout the field, uncertainty in damage location, and uncertainty in the effectiveness of various mitigation strategies.

For example, we are often forced to model the mechanical behavior of entire geologic horizons or multiple vertical intervals based on very limited (or non-existent) core data. The same is true for modeling permeability and porosity variations across a field. Therefore, an appropriate procedure is to perform parametric simulations for a range of potential mechanical and flow properties and to establish probabilities for expected response. Such techniques are used with increasing frequency in the oil and gas industry to estimate production and recoverable reserves, and they can also be applied to estimate casing damage risks and potential effectiveness of various mitigation strategies.

To illustrate this process, consider a simple example to estimate compression damage risks for a sample reservoir using the analytical expressions provided in equation 4. Table 1 presents a set of assumed reservoir and material property variations.   The most likely parameter estimates, designated in the P50 column, are used to provide baselines risk estimates.   We vary each parameter by estimating an approximate low value (P10) and an approximate high value (P90).   That is, we select a low-end value for which there is a 10% probability that actual parameter is lass than the P10 value, and we select a high-end estimate for which there is only a 10% probability that actual parameter is greater than the P90 value.

Table 1. Sample Input Table for Sensitivity Analysis

Input Parameters	P10	P50	P90
Formation Depth (ft below mudline)	1.40E+04	1.60E+04	1.80E+04
Areal Extent (acres)	2.00E+03	4.00E+03	6.00E+03
Gross Formation Thk. (ft)	3.00E+02	4.00E+02	6.00E+02
Net Sand/Gross ratio	6.50E-01	7.50E-01	9.00E-01
Sand Compaction (1/psi)	1.10E-06	3.30E-06	6.60E-06
Shale Compaction (1/psi)	1.00E-07	3.30E-07	1.00E-06
Poisson's Ratio	1.50E-01	2.50E-01	3.50E-01
Pressure Drawdown (psi)	2.00E+03	2.50E+03	3.00E+03
Well Inclination (deg from vertical)	1.00E+01	2.00E+01	4.50E+01
Overburden Young's Modulus (psi)	5.00E+05	1.00E+06	1.50E+06

Table 2 presents a summary of calculated axial strain estimates for the range of assumed input parameters specified in Table 1.   The baseline axial strain, for which all input parameters take on their P50 value, is on the order of 0.5%. The low-end estimate is about 0.2% when the sand compaction coefficient is minimum and the high-end estimate is about 1.1% when the sand compaction coefficient is greatest.   Axial strain sensitivity to various input parameters is illustrated graphically in Figure 15.

Table 2. Sensitivity of axial strain estimates to variable input parameter

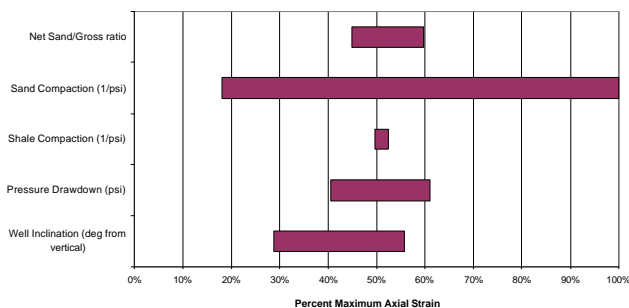| Baseline Axial Strain		5.65E-03	
Axial Strain Sensitivity	**P10**	**P50**	**P90**
Net Sand/Gross ratio	4.99E-03	5.65E-03	6.63E-03
Sand Compaction (1/psi)	2.00E-03	5.65E-03	1.11E-02
Shale Compaction (1/psi)	5.52E-03	5.65E-03	5.83E-03
Pressure Drawdown (psi)	4.52E-03	5.65E-03	6.77E-03
Well Inclination (deg from vertical)	6.20E-03	5.65E-03	3.20E-03
Maximum P90 Axial Strain		1.11E-02	

Figure 15. Axial strain estimate sensitivity to variable input data

Analytical or more sophisticated geomechanical models can therefore be applied to estimate appropriate ranges for expected reservoir deformations and to estimate appropriate ranges for mitigation benefits of specific well designs. A decision analysis tree can be assembled to take into account various completion scenarios and costs, well damage risks, and the risk cost associated with loss events.

We illustrate such a process with a simplified example. A simple economic model, using an EXCEL spreadsheet, is presented in Table 3. Input parameters include a baseline completion cost and two alternative higher cost completion scenarios. The initial well damage risk associated with standard completions is defined to be 10%, consistent with parametric reservoir simulations. A risk reduction factor is assigned to each of the alternative completion strategies, consistent with parametric well casing deformation simulations. In this example completion alternative 2 is estimated to reduce damge risk 50% while completion alternative 3 is estimated to reduce damag risk 75%. Risk cost is defined as the probability of a loss event times the cost of that loss event. All of the input parameters can be varied, allowing one to determine the relative sensitivity of economic benefit conclusions to any one or several input parameters.

The model compares the cost of doing nothing new, which is simply the risk cost of potential well damage for the standard completion, with the cost of alternative completion strategies, which is the added cost of the new completion plus the reduced risk cost of potential damage. The cost of well failure is comprised of the loss of production until the well can be replaced, the replacement cost of the well, and the added abandonment costs.

In this simple example we assume that the inflation rate for well completion, oil price, and abandonment costs are not significantly different from the monetary inflation rate, so that it is sufficient to express all values and compare future costs in today's dollars. This could be easily modified, but will not change results by more than a few percent. We further assume that a damaged well will be identified and replaced within 60 days, that the average production of a well is 300 barrels per day, and that the average price is on the order of 20 dollars per barrel. Each of these parameters can be changed within the model. The results for this specific scenario suggest that the added benefits of alternative completion strategies to mitigate damage do not outweigh the added costs, given the range of uncertainty in risk and benefits. For this example the operator may choose not to modify well designs, but at the same time may discount expected recoverable reserves or return on investment by the total risk cost for all wells when assessing overall field development economics.

Table 3. Simplified economic decision tree example to assess alternative mitigation strategies

Model Input Parameters

Completion #1 Cost	1800000	dollars	Initial damage risk	0.10
Completion #2 Cost	1950000	dollars	Risk reduction	0.50
Completion #3 Cost	2200000	dollars	Risk reduction	0.75
Avg Daily Production	300	bbls/day		
Price per barrel	20	dollars		
Replacement Time	60	days		
Abandonment Cost	200,000	dollars		

				Damage Cost	Risk Cost
				Replacement Well	1800000	$180,000
	Well Damage Risk	0.1		Lost Production	360000	$36,000
				Abandonment Cost	200,000	$20,000
Completion #1 Added Cost	0					$0
				Total Risk Cost		**$236,000**
				Replacement Well	1950000	$97,500
	Well Damage Risk	0.05		Lost Production	360000	$18,000
				Abandonment Cost	200,000	$10,000
Completion #2 Added Cost	150000					$150,000
				Total Risk Cost		**$275,500**
				Replacement Well	2200000	$55,000
	Well Damage Risk	0.025		Lost Production	360000	$9,000
				Abandonment Cost	200,000	$5,000
Completion #2 Added Cost	400000					$400,000
				Total Risk Cost		**$469,000**

Summary and Conclusions

In this paper we have summarized reservoir compaction and casing damage mechanics and field observations, and we have described geomechanical modeling techniques of varying complexity to assess deformations at the reservoir scale and casing damage at the wellbore scale.   We have also discussed decision analysis techniques to compare the costs and benefits of alternative completion strategies to mitigate casing damage risks, given the inherent uncertainty in modeling input data, damage location, and mitigation effectiveness.   The various techniques have been illustrated with real field examples from around the world.   Our investigations to date support the following conclusions and observations:

1. Critical casing damage mechanisms observed in a variety of structural settings worldwide include 1) overburden shear damage on localized horizontal planes; 2) shearing at the top of production and injection intervals; 3) compression and buckling damage within the production interval primarily around perforations.
2. Analytical solutions are readily available to estimate compaction, subsidence, and casing damage risks.   These should be applied as initial screening tools at an early stage in reservoir development planning.   They can also be applied to estimate relative risks for various well locations and trajectories.
3. Geomechanical models of increasing complexity, including two-dimensional and three dimensional finite element type techniques have been used with good success to assess formation deformation and casing damage risks in several reservoirs.
4. Three dimensional geomechanical models at the wellbore scale are required to evaluate shearing deformation on specific well designs, and can be used to assess damage mitigation effectiveness for varying completion strategies.
5. An economic decision tree model can be applied to compare the costs and benefits of alternative well designs, while taking into account inherent uncertainties in model input data, well damage location, and the effectiveness of various mitigation strategies.

Acknowlegements

References

1. Bruno, M.S. (1992), "Subsidence-Induced Well Failure", SPE Drilling Engineering, June, 1992, pp. 148-152.
2. Bruno, M.S. and Bovberg, C.A.: Reservoir Compaction and Surface Subsidence Above the Lost Hills Field, California, Proc. 33rd U.S. Symp. Rock Mech., June 3-5, 1992, pp. 263-272.
3. Cernocky, E.P. and F.C. Scholibo (1995), "Approach to Casing Design for Service in Compacting Reservoirs", SPE 30522, presented at the SPE Annual Technical Conference & Exhibition in Dallas, USA, 22-25 Oct., 1995.
4. Dale, B.A. et al. (1996), "A Case History of Reservoir Subsidence and Wellbore Damage Management in the South Belridge Diatomite Field", paper SPE 35658 presented at the 1996 SPE Western Regional Mtg., Anchorage, 22-24 May.
5. Dusseault, M.B., Bruno, M.S., and Barrera, J.: "Casing Shear: Causes, Cases, Cures", SPE 48864 presented at SPE Int. Conf. and Exhibit, Beijing, China, 2-6 November, 1998.
6. Frame, R.G. (1952), "Earthquake Damage, Its Cause and Prevention in the Wilmington Oil Field", California Oil Fields, Thirty-eighth Annual Report, Dept. of Natural Resources, Division of Oil and Gas, California.
7. Fredrich, J.T., Arguello, J.G., Thorne, B.J., Deitrick, G.L., de Roufignac, E.P., Myer, L.R. and Bruno, M.S., (1996): Three-dimensional geomechanical simulation of reservoir compaction and implications for well failures in the Belridge Diatomite, SPE 36698, Proceedings of the 1996 SPE Ann. Mtg, Denver, Colorado, October 6-9, pp. 195-209.
8. Fredrich, J.T., Holland, J.F., Fossum, A.F., and Bruno, M.S.: "One-way Coupled Reservoir-Geomechanical Modeling of the Lost Hills Oil Field, California", in Proc. 38th US Rock Mechanics Symposium, Washington D.C., July 7-10, 2001.
9. Geertsma, J.: "A numerical Technique for Predicting Subsidence Above Compacting Reservoirs, Based on the Nucleus of Strain Concept", Verhandelingen Kon. Ned. Geol. Mijnbouwk., Vol 28, 1973, pp. 63-78.
10. Gronseth, J.M.: "Geomechanics Monitoring of Cyclic Steam Stimulation Operations in the Clearwater Formation", *Rock at Great Depth,* Maury & Foumaintraux (eds), Balkema, Rotterdam, pp. 1393-1398.
11. Hilbert, L.B., Fredrich, J.T., Bruno, M.S., Deitrick, G.L., and de Rouffignac, E. P., (1996): Two-dimensional nonlinear finite element analysis of well damage due to reservoir compaction, well-to-well interactions, and localization on weak layers, Proc. of the 2nd North Am. Rock Mech. Symp., Quebec, Canada, 19-21, June, 1996, pp. 1863-1870.
12. McCauley, T.V. , "Planning Workovers in Wells with Fault-damaged Casing, South Pass Block 27 Field,"   J. Pet. Tech., (July, 1974).
13. Poland, J.F. and Davis, G.H.: "Land Subsidence Due to Withdrawal of Fluids", in *Reviews in Engineering Geology*, Vol II, D.J. Varnes and G. Kiersch ed., Geological Society of America, 1969.
14. Schwall, G.H. and C.A. Denney, "Subsidence Induced Casing Deformation Mechanisms in the Ekofisk Field", Eurock 94 -- SPE/ISRM Rock Mechanics in Petroleum Engineering, Balkema, Rotterdam, 1994, pp. 507-515.
15. Sen, B.: "Note on Stresses Produced by Nuclei of Thermo-elastic Strain in a Semi-infinite Elastic Solid", Quart. Appl. Math., Vol. VII, No. 4, 1951, pp. 365-369.
16. Yudovich, A.. Chin, L.Y. and Morgan, D.R.: "Casing Deformation in Ekofisk," J. Pet. Tech. (July, 1989)